INTERNATIONAL JOURNAL OF COMPUTATIONAL MATHEMATICAL IDEAS
ISSN: 0974-8652

Design and analysis of Modified Single Input Multiple Output DC-DC Converter interfaced with PV system

Ms. Harini. Voruganti[1] **Mr. A. Madhu mohan reddy**[2]
[1]*PG Student* [2]*Assistant Professor*
[1,2]*Department of Electrical and Electronics Engineering*
[1,2]*Mallareddy Engineering College, Maisammaguda, Hyderabad, JNTUH, TS, India*

Published in Volume 12, Issue 1 Jul - Aug: 2016, Page No: 63204 to 63209

***Abstract*— The point of this study is to build up a high-efficiency single-input multiple output (SIMO) dc–dc converter. The proposed converter can boost the voltage of a low-voltage input power source to a controllable high-voltage dc bus and middle voltage output terminals. The high-voltage dc bus can take as the principle power for a high-voltage dc load or the front terminal of a dc–ac inverter. Also, center voltage output terminals can supply powers for individual center voltage dc loads or for charging helper power sources (e.g., battery modules). In this study, a coupled-inductor based dc–dc converter plan uses one and only power switch with the properties of voltage clipping and delicate exchanging, and the comparing gadget particulars are enough outlined. Here in place of DC source we are interfacing PV system and is validated through simulation results using MATLAB/ Simulink Software.**

***Index Terms*—Coupled inductor, high-efficiency power conversion, single-input multiple-output (SIMO) converter, soft switching, voltage clamping.**

I.INTRODUCTION

IN ORDER to protect the natural environment on the earth, the development of clean energy without pollution has the major representative role in the last decade [1]–[3]. By dealing with the issue of global warming, clean energies, such as fuel cell (FC), photovoltaic, and wind energy, etc., have been rapidly promoted. Due to the electric characteristics of clean energy, the generated power is critically affected by the climate or has slow transient responses, and the output voltage is easily influenced by load variations [4]–[6]. Besides, other auxiliary components, e.g., storage elements, control boards, etc., are usually required to ensure the proper operation of clean energy. For example, an FC-generation system is one of the most efficient and effective solutions to the environmental pollution problem [7]. In addition to the FC stack itself, some other auxiliary components, such as the balance of plant (BOP) including an electronic control board, an air compressor, and a cooling fan, are required for the normal work of an FC generation system [8], [9]. In other words, the generated power of the FC stack also should satisfy the power demand for the BOP. Thus, various voltage levels should be required in the power converter of an FC generation system. In general, various single-input single-output dc–dc converters with different voltage gains are combined to satisfy the requirement of various voltage levels, so that its system control is more complicated and the corresponding cost is more expensive. The motivation of this study is to design a single-input multiple-output (SIMO) converter for increasing the conversion efficiency and voltage gain, reducing the control complexity, and saving the manufacturing cost. Patra et al. [9] presented a SIMO dc–dc converter capable of generating buck, boost, and inverted outputs simultaneously. However, over three switches for one output were required. This scheme is only suitable for the low output voltage and power application, and its power conversion is degenerated due to the operation of hard switching. Nami et al. proposed a new dc–dc multi-output boost converter, which can share its total output between different series of output voltages for low- and high-power applications. Unfortunately, over two switches for one output were required, and its control scheme was complicated. Besides, the corresponding output power cannot supply for individual loads independently. Chen et al.investigated a multiple-output dc–dc converter with shared zero-current switching (ZCS) lagging leg. Although this converter with the soft-switching property can reduce the switching losses, this combination scheme with three full-bridge converters is more complicated, so that the objective of high-efficiency power conversion is difficult to achieve, and its cost is inevitably increased. This study presents a newly designed SIMO converter with a coupled inductor. The proposed converter uses one power switch to achieve the objectives of high-efficiency power conversion, high step-up ratio, and different output voltage levels. In the proposed SIMO converter, the techniques of soft switching and voltage clamping are adopted to reduce the switching and conduction losses via the

utilization of a low-voltage-rated power switch with a small RDS(on) . Because the slew rate of the current change in the coupled inductor can be restricted by the leakage inductor, the current transition time enables the power switch to turn ON with the ZCS property easily, and the effect of the leakage inductor can alleviate the losses caused by the reverse-recovery current. Additionally, the problems of the tray inductance energy and reverse-recovery currents within diodes in the conventional boost converter also can be solved, o that the high-efficiency power conversion can be achieved. The voltages of middle-voltage output terminals can be appropriately adjusted by the design of auxiliary inductors; the output voltage of the high-voltage dc bus can be stably controlled by a simple proportional-integral (PI) control. This study is mainly organized into five sections. Following the introduction, the converter design and analyses are given in Section II. In Section III, the design considerations of the proposed SIMO converter are discussed in detail. Section IV provides simulation results to validate the effectiveness of the proposed converter in practical applications. Finally, some conclusions are drawn in Section V.

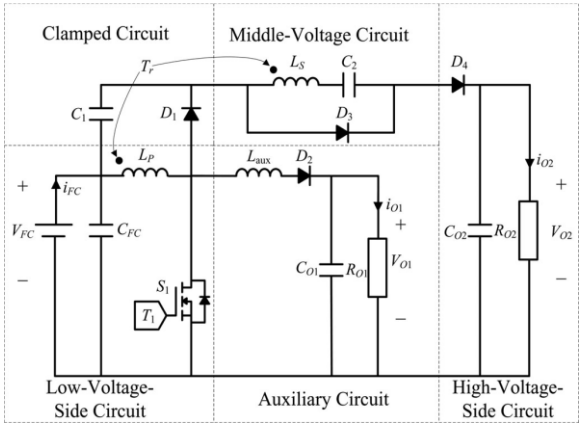

Fig. 1. System configuration of high-efficiency single-input multiple-output (SIMO) converter.

II. CONVERTER DESIGN AND ANALYSES

The system configuration of the proposed high-efficiency SIMO converter topology to generate two different voltage levels from a single-input power source is depicted in Fig. 1. This SIMO converter contains five parts including a low-voltage-side circuit (LVSC), a clamped circuit, a middle-voltage circuit, an auxiliary circuit, and a high-voltage-side circuit (HVSC). The major symbol representations are summarized as follows. VFC (iFC) and VO1 (iO1) denote the voltages (currents) of the input power source and the output load at the LVSC and the auxiliary circuit, respectively; VO2 and iO2 are the output voltage and current in the HVSC. CFC, CO1 , and CO2 are the filter capacitors at the LVSC, the auxiliary circuit, and the HVSC, respectively; C1 and C2 are the clamped and middle-voltage capacitors in the clamped and middle-voltage circuits, respectively. LP and LS represent individual inductors in the primary and secondary sides of the coupled inductor Tr , respectively, where the primary side is connected to the input power source; Laux is the auxiliary circuit inductor. The main switch is expressed as S1 in the LVSC; the equivalent load in the auxiliary circuit is represented as RO 1 , and the output load is represented as RO 2 in the HVSC. The corresponding equivalent circuit given in Fig. 2 is used to define the voltage polarities and current directions. The coupled inductor in Fig. 1 can be modeled as an ideal transformer including the magnetizing inductor Lmp and the leakage inductor Lkp in Fig. 2. The turns ratio N and coupling coefficient k are defined as

$$N = N2/N1 \quad (1)$$

$$K = Lmp/(Lkp + Lmp) = Lmp/LP \quad (2)$$

where N1 and N2 are the winding turns in the primary and secondary sides of the coupled inductor Tr . Because the voltage gain is less sensitive to the coupling coefficient and the clamped capacitor C1 is appropriately selected to completely absorb the leakage inductor energy [13], the coupling coefficient could be simply set at one (k = 1) to obtain Lmp = LP via (2). In this study, the following assumptions are made to simplify the converter analyses: 1) The main switch including its body diode is assumed to be an ideal switching element; and 2) The conduction voltage drops of the switch and diodes are neglected

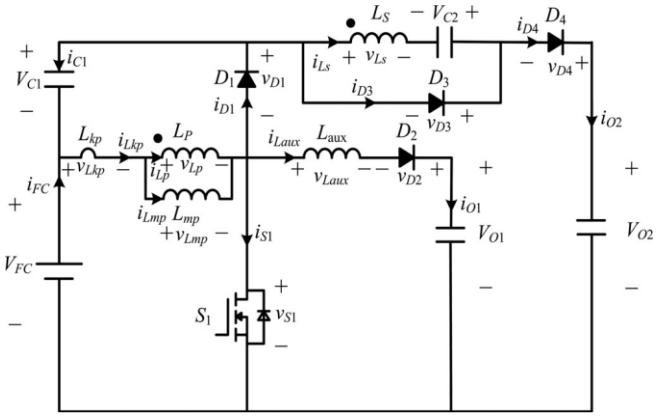

Fig.2. Equivalent circuit

A. Operation Modes

The topological modes in one switching cycle are illustrated in Fig. 3,4,5,6,7,8 respectively.

1) Mode 1 (t0 –t1) [Fig. 3]: In this mode, the main switch S1 was turned ON for a span, and the diode D4 turned OFF. Because the polarity of the windings of the coupled inductor Tr is positive, the diode D3 turns ON. The secondary current iLs reverses and charges to the middle voltage capacitor C2 . When the auxiliary inductor Laux releases its stored energy completely, and the diode D2 turns OFF, this mode ends.

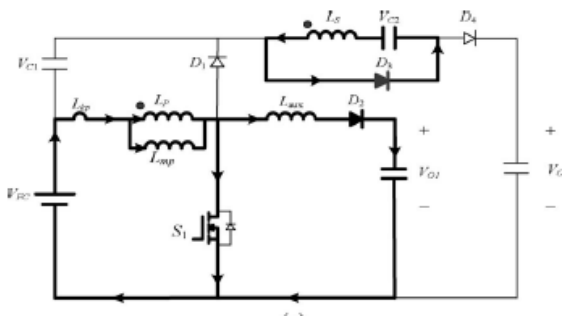

Fig.3. Circuit diagram of Mode 1 operation

2) Mode 2 (t1 –t2) [Fig. 4(b)]: At time t = t1 , the main switch S1 is persistently turned ON. Because the primary inductor LP is charged by the input power source, the magnetizing current iLmp increases gradually in an approximately linear way. At the same time, the secondary voltage vLs charges the middle-voltage capacitorC2 through the diode D3 . Although the voltage vLmp is equal to the input voltage VFC both at modes 1 and 2, the ascendant slope of the leakage current of the coupled inductor (diLkp /dt) at modes 1 and 2 is different due to the path of the auxiliary circuit. Because the auxiliary inductor Laux releases its stored energy completely, and the diode D2 turns OFF at the end of mode 1, it results in the reduction of diLkp /dt at mode 2.

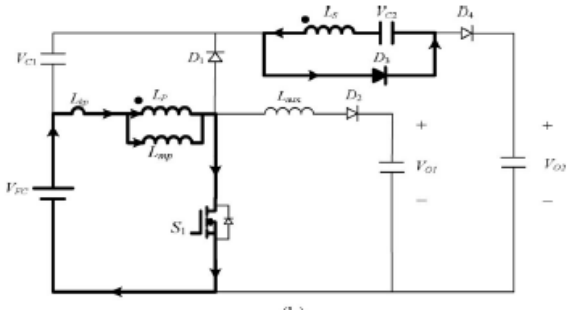

Fig.4. Circuit diagram of Mode 2 operation

3) Mode 3 (t2 –t3) [Fig. 4(c)]: At time t = t2 , the main switch S1 is turned OFF. When the leakage energy still released from the secondary side of the coupled inductor, the diode D3 persistently conducts and releases the leakage energy to the middle-voltage capacitor C2 . When the voltage across the main switch vS 1 is higher than the voltage across the clamped capacitor VC 1 , the diode D1 conducts to transmit the energy of the primary-side leakage inductor Lkp into the clamped capacitor C1 . At the same time, partial energy of the primary-side leakage inductor Lkp is transmitted to the auxiliary inductor Laux, and the diode D2 conducts. Thus, the current iL aux passes through the diode D2 to supply the power for the output load in the auxiliary circuit. When the secondary side of the coupled inductor releases its leakage energy completely, and the diode D3 turns OFF, this mode ends.

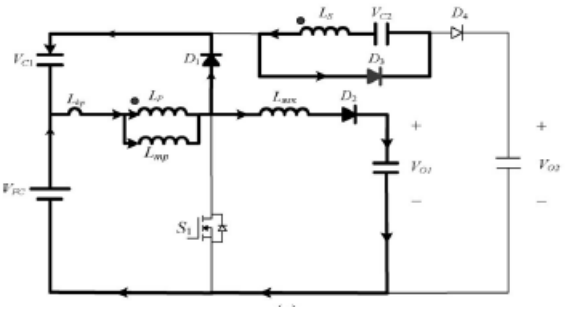

Fig.5. Circuit diagram of Mode 3 operation

4) Mode 4 (t3 –t4) [Fig. 4(d)]: At time t = t3 , the main switch S1 is persistently turned OFF. When the leakage energy has released from the primary side of the coupled inductor, the secondary current iLS is induced in reverse from the energy of the magnetizing inductor Lmp through the ideal transformer, and flows through the diode D4 to the HVSC. At the same time, partial energy of the primaryside leakage inductor Lkp is still persistently transmitted to the auxiliary inductor Laux, and the diode D2 keeps to conduct. Moreover, the current iL aux passes through the diode D2 to supply the power for the output load in the auxiliary circuit.

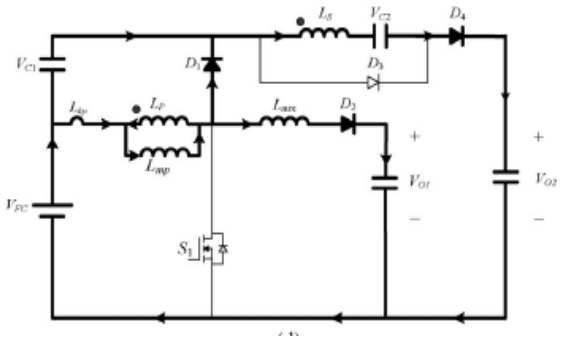

Fig.5. Circuit diagram of Mode 4 operation

5) Mode 5 (t4 –t5) [Fig. 4(e)]: At time t = t4 , the main switch S1 is persistently turned OFF, and the clamped diode D1 turns OFF because the primary leakage current iLkp equals to the auxiliary inductor current iL aux. In this mode, the input power source, the primary winding of the coupled inductor Tr , and the auxiliary inductor Laux connect in series to supply the power for the output load in the auxiliary circuit through the diode D2 . At the same time, the input power source, the secondary winding of the coupled inductor Tr , the clamped capacitor C1 , and the middle voltage capacitor (C2) connect in series to release the energy into the HVSC through the diode D4 .

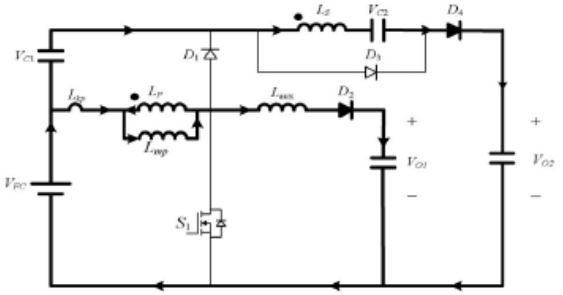

Fig.7. Circuit diagram of Mode 5 operation

6) Mode 6 (t5 –t6) [Fig. 4(f)]: At time t=t5 , this mode begins when the main switch S1 is triggered. The auxiliary inductor current iL aux needs time to decay to zero, the diode D2 persistently conducts. In this mode, the input power source, the clamped capacitor C1 , the secondary winding of the coupled inductor Tr , and the middle-voltage capacitor C2 still connect in series to release the energy into the HVSC through the diodeD4 . Since the clamped diodeD1 can be selected as a low-voltage Schottky diode, it will be cut off promptly without a reverse-recovery current. Moreover, the rising rate of the primary current iLkp is limited by the primary-side leakage inductor Lkp . Thus, one cannot derive any currents from the paths of the HVSC, the middle-voltage circuit, the auxiliary circuit, and the clamped circuit. As a result, the main switch S1 is turned ON under the condition of ZCS and this soft-switching property is helpful for alleviating the switching loss. When the secondary current iLS decays to zero, this mode ends. After that, it begins the next switching cycle and repeats the operation in mode 1.

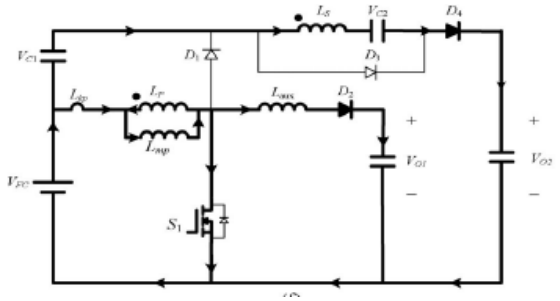

Fig.8. Circuit diagram of Mode 6 operation

In general, a dc–dc converter operated at the continuous conduction mode (CCM) can provide a low ripple current for protecting the energy source. In the proposed SIMO converter, it is operated at the CCM due to the design of the auxiliary inductor. The coupled inductor is charged by the input power source when the main switch is turned ON, and the coupled inductor releases its energy to the auxiliary inductor when the main switch is turned OFF until the energy balance of the coupled inductor and the auxiliary inductor is established.

III. DESIGN CONSIDERATIONS

By defining the minimum and maximum output powers in the auxiliary circuit and the HVSC as (*P*1 min, *P*1 max) and (*P*2 min, *P*2 max), respectively. In the case of resistive loads ,The minimum resistances connected at the auxiliary circuit and the HVSC can be expressed as

$$R_{01min} = \frac{G_{vl}2 * Vfc2}{P_{1max}}$$

$$R_{02min} = \frac{G_{vH}2 * Vfc2}{P_{2max}}$$

The maximum resistances connected at the auxiliary

circuit and the HVSC as

$$R_{01max} = \frac{G_{vl}2 * Vfc2}{P_{1min}}$$

$$R_{02min} = \frac{G_{vl}2 * Vfc2}{P_{2max}}$$

The limit for Laux can be calculated as

*L*aux < 0.5*d*1*RO*1*TS*

The voltage across the main switch S1 can be represented as

*vS*1 = *VC*1 + *V*FC = [1/(1 − *d*1)]*V*FC,

The capacitor C01 can be calculated as

*CO*1 = (*d*1 − *dx*)/[(*RO*1*fS*)(Δ*VO*1/*VO*1)]

The capacitor C02 can be calculated as

*CO*2 = *d*1/[(*RO*2*fS*)(Δ*VO*2/*VO*2)]

The proposed converter resonant frequencies are calculated as

$$f_{o1} = 1/2\pi\sqrt{LpC1}$$

IV. SIMULATION & RESULTS

The simulation of modified single input multi output dc-dc converter is done using MATLAB/SIMULINK software and the results are as follows. The simulation results are discussed and compared with the output voltage results. single input multi output dc-dc converter is simulated by using pulse width modulation technique.PWM technique is connected with input of the MOSFET gate terminal.

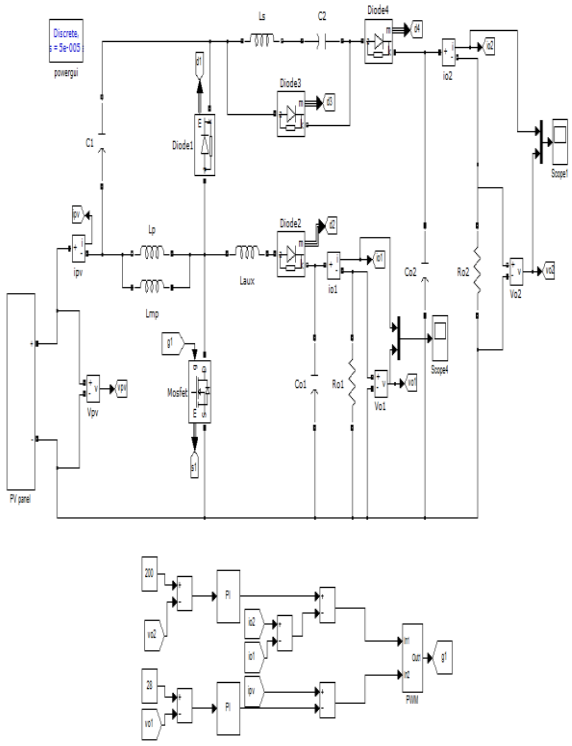

Fig.9. Simulation diagram for SIMO DC-DC Converter with PV system

Modified Single Input Multi Output DC-DC Converter can boost the voltage low voltage input source .That input voltage is 12V to controllable Boost the voltage is 14V,and High voltage is 200V, and middle output-voltage is 20-24V.The auxiliary inductor value is 2µH. And that capacitor value is c1=85µf, c2 value is 10µf.One coupled inductor is used. The primary of the coupled inductor is 2µH.secondary of the coupled inductor is 75µH.

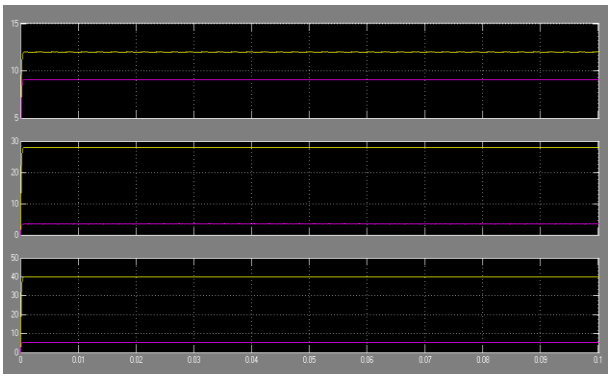

Fig.10.Voltage and current responses of SIMO converter with 200-W output power.

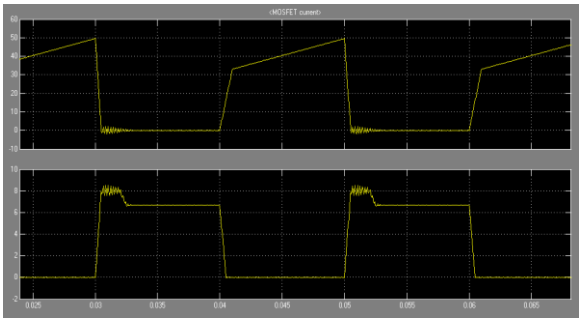

Fig.11.Voltage and current responses across Switch in SIMO converter

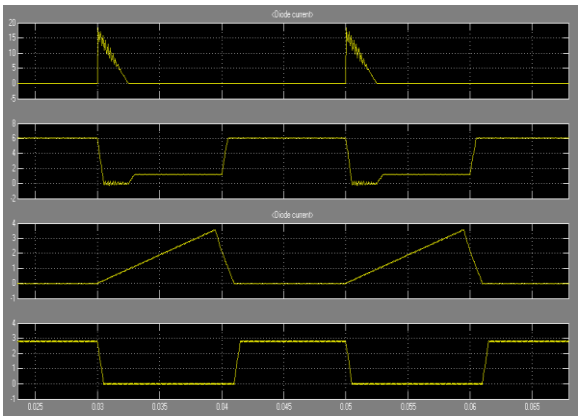

Fig.12.Voltage and current responses across Diode(D1,D2) in SIMO converter

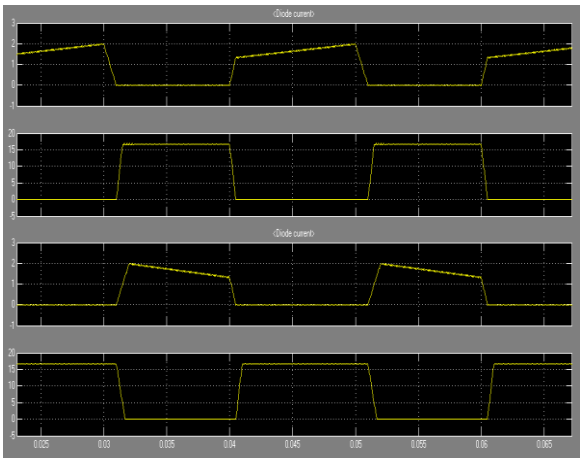

Fig.13.Voltage and current responses across Diode(D3,D4) in SIMO converter

V.CONCLUSION

This study has successfully developed a high-efficiency SIMO dc–dc converter, and this coupled-inductor-based converter was applied well to a single-input power source plus two output terminals composed of an auxiliary battery module and a high-voltage dc bus with high efficiency. The simulation result shows the single input power source is converted to multiple output terminals. This topology adopts only one power switch to achieve the objective of multiple output with power conversion.

REFERENCES

[1] Chen.Y and Kang.Y;“A full regulated dual-output dc-dc converter with special-connected two transformers (SCTTs) cell and complementary pulse width modulation-PFM(CPWM-PFM),” IEEE Trans. Power Electron., vol. 25, no. 5, pp. 1296–1309, May 2010

[2] Chen.Y, Kang.Y, Nie.S, and Pei.X; “The multiple-output DC–DC converter with shared ZCS lagging leg,” IEEE Trans. Power Electron., vol. 26, no. 8, pp. 2278–2294, Aug. 2011.

[3] Ellis M.W,.VonSpakovsky M.R, and Nelson D.J;“Fuel cell systems: Efficient, flexible energy conversion for the 21 st century,”Proc. IEEE, vol. 89, no. 12, pp. 1808– 1818, Dec. 2001

[4] GaminiJayasinghe.S.D, MahindaVilathgamuwa.D, and MadawalaU.K,;“Diode-clamped three-level inverterbased bat-tery/supercapacitor direct integration schemefor renewable energy sys-tems,” IEEE Trans. Power Electron., vol. 26, no. 6, pp. 3720–3729, Dec. 2011.

[5] Kim.T, Vodyakho.O, and Yang.J; “Fuel cell hybrid electronic scooter,”IEEE Ind. Appl. Mag., vol. 17, no. 2, pp. 25–31, Mar./Apr. 2011.

[6] Gao.F, Blunier.B, Sim.M.G˜ oes, and Miraoui.A; “PEM fuel cell stack modeling for real-time emulation in hardware-in-the-loop application,”IEEE Trans. Energy Convers., vol. 26, no. 1, pp. 184–194, Mar. 2011

[7] Kirubakaran.A, Jain., and NemaR.K; “DSP-controlled power elec-tronic interface for fuel-cell-based distributed generation,” IEEE Trans. Power Electron., vol. 26, no. 12, pp. 3853–3864, Dec. 2011.

[8] Kim.J.K, Choi.S.W, and Moon.G.W; “Zero-voltage switching post regulation scheme for multi output forward converter with synchronous switches,” IEEE Trans. Ind. Electron., vol. 58, no. 6, pp. 2378–2386,Jun. 2011

[9] Liu.B, Duan.S, and Cai.T,; “Photovoltaic dc-buildingmodule- based BIPV system-concept and design considerations,” IEEE Trans. Power Electron., vol. 26, no. 5, pp. 1418–1429, May 2011.